Naval Surface Warfare Center
Carderock Division
West Bethesda, MD 20817-5700

NSWCCD-70-TR–2000/201 December 2000

Signatures Directorate

Research and Development Report

The Role of Coupling Forms and of Coupling Strengths on the Induced Loss Factor

by

G. Maidanik and K. J. Becker

NSWCCD-70-TR–2000/201

REPORT DOCUMENTATION PAGE

Form Approved
OMB No. 0704-0188

1. REPORT DATE *(DD-MM-YYYY)* 14-Dec-2000	**2. REPORT TYPE** Final	**3. DATES COVERED** *(From - To)* -
4. TITLE AND SUBTITLE The Role of Coupling Forms and Coupling Strengths on the Induced Loss Factor		**5a. CONTRACT NUMBER**
		5b. GRANT NUMBER
		5c. PROGRAM ELEMENT NUMBER
6. AUTHOR(S) G. Maidanik and K. J. Becker		**5d. PROJECT NUMBER**
		5e. TASK NUMBER
		5f. WORK UNIT NUMBER
7. PERFORMING ORGANIZATION NAME(S) AND ADDRESS(ES) AND ADDRESS(ES) Naval Surface Warfare Center, Carderock Division, 9500 Macarthur Boulevard, West Bethesda, MD 20817-5700		**8. PERFORMING ORGANIZATION REPORT NUMBER** NSWCCD-70-TR-2000/201
9. SPONSORING / MONITORING AGENCY NAME(S) AND ADDRESS(ES)		**10. SPONSOR/MONITOR'S ACRONYM(S)**
		11. SPONSOR/MONITOR'S REPORT NUMBER(S)

12. DISTRIBUTION / AVAILABILITY STATEMENT
Approved for public release; Distribution is unlimited.

13. SUPPLEMENTARY NOTES

14. ABSTRACT
The role played by the coupling forms and coupling strengths in determining the induced loss factor of a master oscillator due to its coupling to a set of satellite oscillators is assessed and evaluated.

15. SUBJECT TERMS

16. SECURITY CLASSIFICATION OF:			**17. LIMITATION OF ABSTRACT**	**18. NUMBER OF PAGES**	**19a. NAME OF RESPONSIBLE PERSON** G. Maidanik
a. REPORT UNCLASSIFIED	**b. ABSTRACT** UNCLASSIFIED	**c. THIS PAGE** UNCLASSIFIED	SAR	0	**19b. TELEPHONE NUMBER** *(include area code)* 301-227-1292

Standard Form 298 (Rev. 8-98)
Prescribed by ANSI Std. Z39.18

Preface

Due to a temporary health condition, the paper entitled "Weak and strong couplings between a master oscillator and a set of satellite oscillators" was not delivered at the ASA 140th Meeting held at Newport Beach, CA, during the period 3-8 December 2000. However, the material to be presented is deemed, by the authors, worthwhile. Here it is offered in the form of a report, so that those who are interested will not remain deprived, and those who are not interested may remain blissfully ignorant, and just ignore this report.

The report is largely written in the manner in which the original presentation would have been given. Nonetheless, the title is changed to reflect more closely the current intent of the authors; after all the title and abstract were done months ago. Of course, some liberty is taken with regards to time. Some of the points and some of the exhibits that would have had to be cut are herein included. Nonetheless, the liberty of time is exercised with caution. Also, the reader will find that the viewgraphs are not in mint condition; the viewgraphs are preserved in their original forms. However, almost all letters are in typed form. (One of the authors was once warned, by a University Professor, no less, that hand-written letters are not acceptable to him. If he sees them in viewgraphs, he ignores the viewgraphs, period, says he. We would hate to be ignored, a priori, by University Professors, whether they are of the "he" or the "she" types [1].)

The material herein is based on, and is an extension to, a recent paper by one of the authors [2]. In addition to reassessing the stiffness control coupling form, the extension consists largely of the inclusion of mass and gyroscopic control coupling forms. Moreover, the extension allows for various coupling strengths; from weak to strong coupling strengths.

We have advanced with the inclusion of viewgraphs that carry graphical curves in colors. We trust that colors are of help. We hope in the future to become more and more colorful. Finally, we appreciate your kind indulgence and interest in reading this report.

Viewgraph 1

The complex consisting of a master oscillator that is coupled to a set of satellite oscillators is sketched in this viewgraph. The couplings are typically defined by a stiffness control term (k_{cr}), a mass control term (m_{cr}) and a gyroscopic coefficient (G_r) [2]. The losses in the complex are cast as stiffness control terms. (See viewgraph.) The stiffness control terms are, in turn, defined by the resonance frequencies (ω_o), (ω_r) and (ω_{cr}), as indicated on the viewgraph. Note that both (ω_r) and (ω_{cr}) are defined with respect to the mass (m_r) of the (r)th satellite oscillator.

the complex

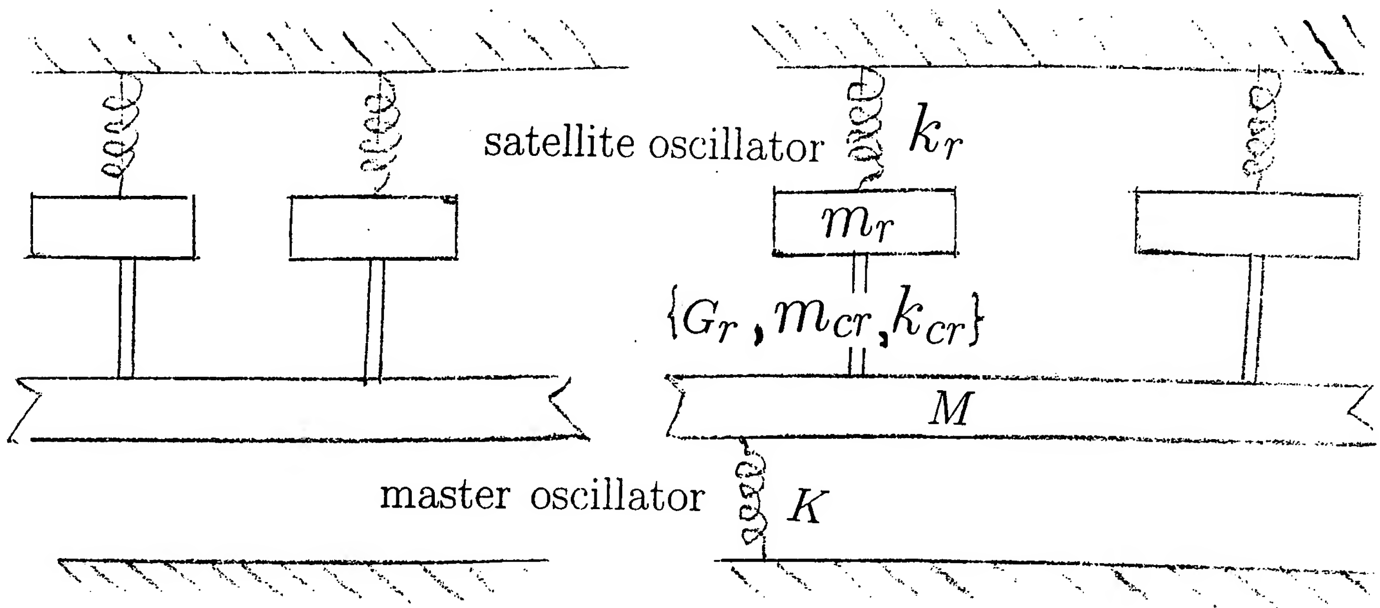

The mass and the stiffness control terms in this complex are related in the forms

$$K = K_o(1 + i\eta_o) \quad ; \quad (K_o/M) = \omega_o^2 \quad ,$$

$$k_r = k_{or}(1 + i\eta_r) \quad ; \quad (k_{or}/m_r) = \omega_r^2 \quad ,$$

$$k_{cr} = k_{ocr}(1 + i\eta_{cr}) \quad ; \quad (k_{ocr}/m_r) = \omega_{cr}^2 \quad ,$$

where the pairs $\{M, K\}$, $\{m_r, k_r\}$, and $\{m_r, k_{cr}\}$ are in reference to the master oscillator, to the (r)th satellite oscillator and to the coupling between them. The parameters (η_o), (η_r), and (η_{cr}) are the corresponding stiffness control loss factors, respectively.

Viewgraph 2

In expressing the linear impedance $Z_o(\omega)$ of a master oscillator that is coupled to a set of (R) satellite oscillators, it is convenient to cast the influence of this coupling by defining an induced reactive factor S(y) and an induced loss factor $\eta_s(y)$ [2, 3]. Here the focus is set largely on the induced loss factor $\eta_s(y)$. The expression for this loss factor is conveniently cast in terms of normalized parameters that specify the master oscillator, the set of satellite oscillators and the couplings between the master oscillator and each member of the set. The expression is dominated by a sum over the satellite oscillators in the set. The normalized coupling parameters are $(z_{cr})^2$, $(\overline{m_{cr}})$ and $(\overline{g_r})$, which are in reference to the stiffness, the mass and the gyroscopic forms, respectively.

It is gratifying to find that the dependence on the gyroscopic parameter $(\overline{g_r})$ is quadratic so that the induced loss factor $\eta_s(y)$ is not dependent on the sign of $(\overline{g_r})$. It is noted, in passing, that the induced reactive factor S(y) is independent of $(\overline{g_r})$ altogether. [One is reminded that the gyroscopic coupling is acting in quadrature to either the mass or stiffness coupling.]

The linear impedance $Z_O(\omega)$ of a master oscillator that is coupled to a set of (R) satellite oscillators may be expressed in the form

$$Z_O(\omega) = Z_O(y) = (i\omega M)\left[1 - (y)^{-2}\left\{[1 - S(y)] + i[\eta_O + \eta_S(y)]\right]\right\}$$

The induced loss factor $\eta_s(y)$ is then

$$\eta_s(y) = -(y)^2 Im\left\{\sum_1^R \overline{m}_r \left[(1+\overline{m}_{cr}) - (z_{rr})^2(1+\eta_{rr})\right]^{-1}\right.$$
$$\left[\left\{(1-(z_r)^2(1+i\eta_r)\right\}\left\{\overline{m}_{cr} - (z_{cr})^2(1+i\eta_{cr})\right\} - (\overline{q}_{cr}/y)^2\right]$$

where the normalization of some of the variables and parameters that define the complex are:

$$y = (\omega/\omega_o) \quad ; \quad x_r = (\omega_r/\omega_o) \quad ; \quad x_{cr} = (\omega_{cr}/\omega_o)$$

$$\overline{m}_{cr} = (m_{cr}/m_r) \quad ; \quad \overline{g}_r = [G_r/(\omega_o m_r)]$$

$$z_{rr} = (x_{rr}/y) \quad ; \quad z_r = (x_r/y) \quad ; \quad z_{cr} = (x_{cr}/y)$$

$$(\overline{q}_{cr}/y)^2 = 4\overline{m}_{cr}(z_{cr})^2(1+i\eta_{cr}) + (\overline{g}_r/y)^2$$

Viewgraph 3

Again, a sketch of the complex is depicted. The normalization of the frequencies by the resonance frequency of the master oscillator (ω_o) is also repeated.

A new concept is introduced: The normalized resonance frequencies (x_r) and (x_{cr}) are rendered similar by defining the stiffness parameters (α_r) and (α_{cr}) ; (α_r) pertaining to the "spring" in the (r)th satellite oscillator and (α_{cr}) pertaining to the "spring" in the coupling of this satellite oscillator to the master oscillator. The combined normalized frequency (x_{rr}) is given by:

$$(x_{rr})^2 = \alpha_r \, (x_r^o)^2 + \alpha_{cr} \, (x_r^o)^2 = (\alpha_r + \alpha_{cr}) \, (x_r^o)^2.$$

The corresponding mass coupling parameter ($\overline{m}_{cr}$) and gyroscopic coupling parameter ($\overline{g}_r$) are also defined [3]. A condition between the stiffness parameters (α_r) and (α_{cr}) and the mass coupling parameter ($\overline{m}_{cr}$) emerges. This condition fixes (x_{rr}); (x_{rr}) is related to the total normalized stiffness in the (r)th satellite oscillator; normalized with respect to the mass (m_r) of that satellite oscillator. The fixed (x_{rr}) is related to the total normalized stiffness to which the mass (m_r) of the (r)th satellite oscillator is subjected when the master oscillator is blocked. The fixed (x_{rr}), as a function of ($\overline{r}$), is displayed in the viewgraph. The normalized discrete or continuous index (r) is designated $\overline{r} = [r \, (R+1)^{-1}]$. The index ($r$) is that assigned to identify the (r)th satellite oscillator and it is further imposed that ($x_{r+1,\, r+1} > x_{r,r}$) and the number of satellite oscillators on either side of the resonance frequency (ω_o) is equal. The choice of the expression for (x_r^o) is selected here to conform to one of the forms recently considered in a paper by one of the authors [2]. The choice for (x_r^o) is not otherwise restricted. A large variety of forms are admissible.

the complex

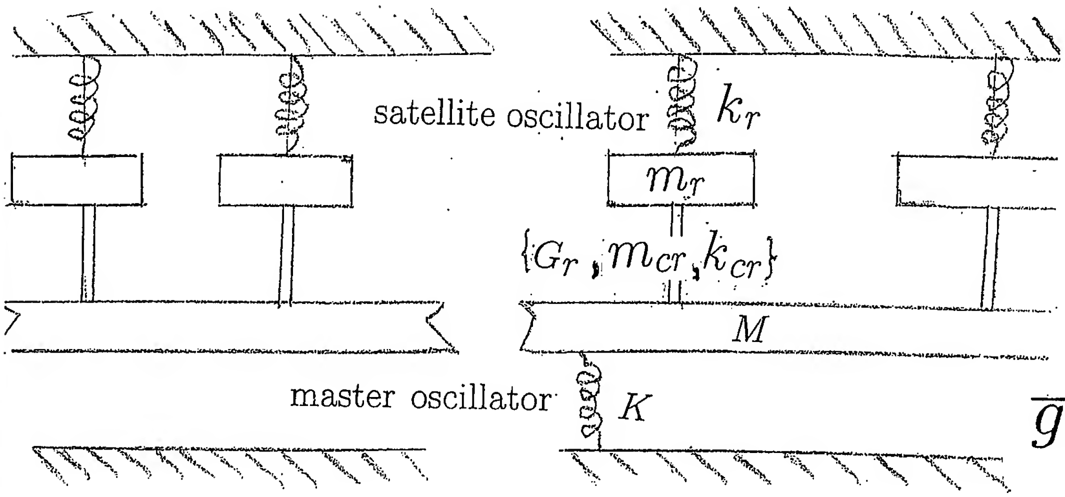

$$y = (\omega/\omega_o)$$

$$x_r = (\omega_r/\omega_o)$$

$$x_{cr} = (\omega_{cr}/\omega_o)$$

$$\overline{g}_r = [G_r/(\omega_o m_r)]$$

$$(x_r) = (\alpha_r)^{1/2}(x_r^o) \quad ; \quad (x_{cr}) = (\alpha_{cr})^{1/2}(x_r^o)$$

$$(x_{rr}) = (\alpha_r + \alpha_{cr})^{1/2}(x_r^o) \quad ; \quad x_r^o = [1 + \{1 - 2\overline{r}\}\gamma(\overline{R})]^{-1/2}$$

$$\overline{r} = r(R+1)^{-1} ; \ \overline{R} = R(R+1)^{-1} \quad ; \quad \gamma(\overline{R}) = [\gamma/(2\overline{R})] \quad ; \quad \gamma < 1$$

$$\overline{m}_{cr} = (m_{cr}/m_r) \ ; \ (\alpha_r + \alpha_{cr}) = (1 + \overline{m}_{cr})$$

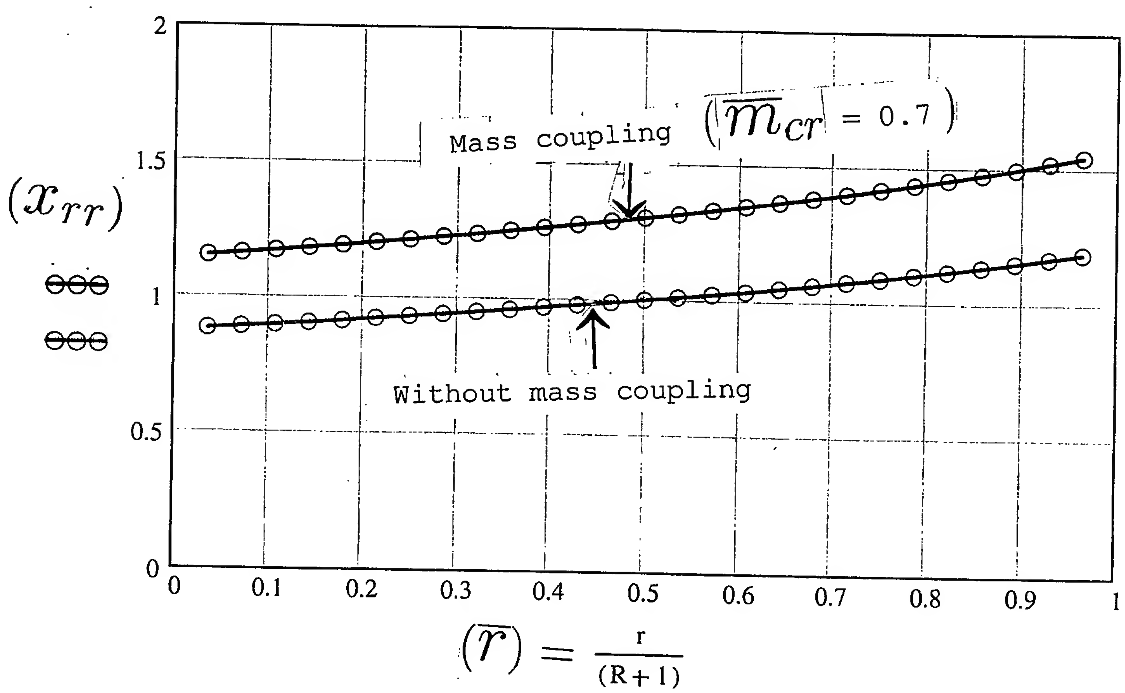

Viewgraph 4

In the literature the common satellite oscillators are depicted as sprung-masses [4-14]. A sprung-mass defines a satellite oscillator that is mass controlled; i.e., $\alpha_r = 0$, and is very strongly coupled to the master oscillator; i.e., $\alpha_{cr} = 1$. What is new in the present effort? In addition to sprung-masses, other types of satellite oscillators and other types of couplings are admitted; e.g., mass and gyroscopic control couplings [3]. Moreover, in all forms of couplings, the coupling strengths may be varied from weak to strong. A variety of coupling forms and their strengths are defined and exemplified in the viewgraph.

Sprung-Masses-stiffness couplings only

$(\alpha_r + \alpha_{cr}) = 1$; $\alpha_{cr} \neq 0$; $\overline{m_{cr}} = 0$; $\overline{g_r} = 0$

	Weak-	Moderate-	Strong-	Couplings
$\alpha_{cr} \simeq$	0.03	0.15	0.75	

Gyroscopic couplings only

$\alpha_r = 1$; $\alpha_{cr} = 0$; $\overline{m_{cr}} = 0$; $\overline{g_r} \neq 0$

	Weak-	Moderate-	Strong-	Couplings
$\overline{g_r} \simeq$	0.03	0.15	0.75	

Mass coupling only

$\alpha_r = (1 + \overline{m_{cr}})$; $\alpha_{cr} = 0$; $\overline{m_{cr}} \neq 0$; $\overline{g_r} = 0$

	Weak-	Moderate-	Strong-	Couplings
$\overline{m_{cr}} \simeq$	0.03	0.15	0.75	

Combination thereof; e.g.,

Stiffness + gyroscopic couplings $[(\alpha_r + \alpha_{cr}) = 1]$

$\alpha_r \neq 0$; $\alpha_{cr} \neq 0$; $\overline{m_{cr}} = 0$; $\overline{g_r} \neq 0$

	Weak-	Moderate-	Strong-	Couplings
$(\alpha_{cr} + \overline{g_r}) \simeq$	0.03	0.15	0.75	

Viewgraph 5

The definition of the modal overlap parameter (b_r) is given in this viewgraph [2, 3].

Under certain assumptions, e.g., $b_r = b_{cr}$, $\alpha_r = \alpha$ and $\alpha_{cr} = \alpha_c$, the loss factor (η_{rr}) may be simply stated. The explicit expression for the loss factor (η_{rr}) of the (r)th satellite oscillator, that is appropriate to the form of (x_r^o) which is defined in Viewgraph 3, is presented. The loss factor (η_{rr}) is directly proportioned to the modal overlap parameter (b_r).

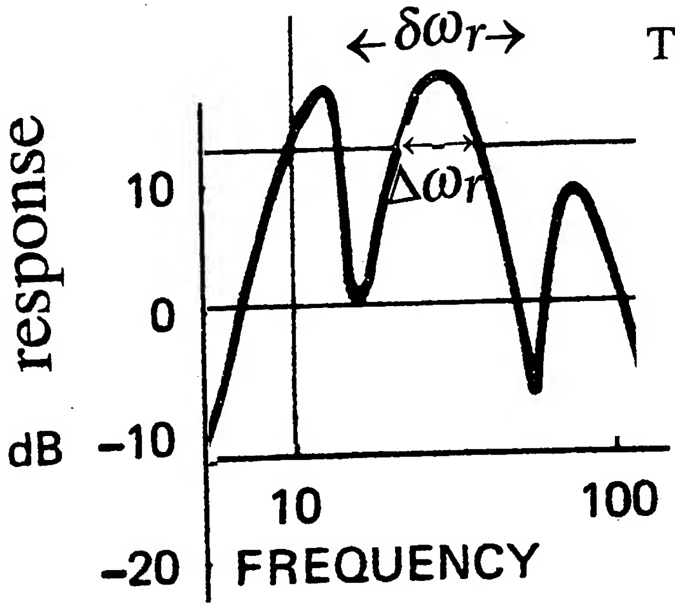

The inverse of the frequency bandwidth ($\delta\omega_r$) is commonly referred to as the *modal density* (n_r)

$$n_r = (\delta\omega_r)^{-1} \quad ; \quad \varepsilon \leq r \leq R+\varepsilon$$

$$\Delta\omega_r = (\omega_r \eta_r) U(r-\varepsilon) U(R+\varepsilon-r) \quad .$$

The ratio (b_r) of these two frequency bandwidths defines a *modal overlap parameter*

$$\{ b_r = (\Delta\omega_r / \delta\omega_r) = (n_r \omega_r \eta_r) \} U(r-\varepsilon) U(R+\varepsilon-r)$$

Loss factor of satellite oscillators

$$\eta_{rr} = b_r [\partial \ln(x_r^o)/\partial r] = (\overline{b}_r)[\gamma(\overline{R})(x_r^o)^2] \ ;$$

$$b_r = b_{cr} \quad ; \quad \overline{b}_r = b_r (R+1)^{-1} \quad ; \quad \alpha_r = \alpha \quad ; \quad \alpha_{cr} = \alpha_c$$

$$\eta_r = \eta_{cr} = \eta_{rr} \quad \text{Independent of couplings}$$

Viewgraph 6

The loss factor (η_{rr}) associated with the (r)th satellite oscillator is presented as a function of the normalized index (r). This normalized index is designated ($\bar{r}$). The loss factor (η_{rr}), as a function of ($\bar{r}$), is depicted in this viewgraph for two values of the modal overlap parameter (b_r) as just defined in Viewgraph 5. These values are (0.1) and (2); they are in the ratio of (20). One recalls that under the specification of the complex here considered, $\eta = \eta_{rr} = \eta_r = \eta_{cr}$ and these loss factors are independent of the forms of the couplings.

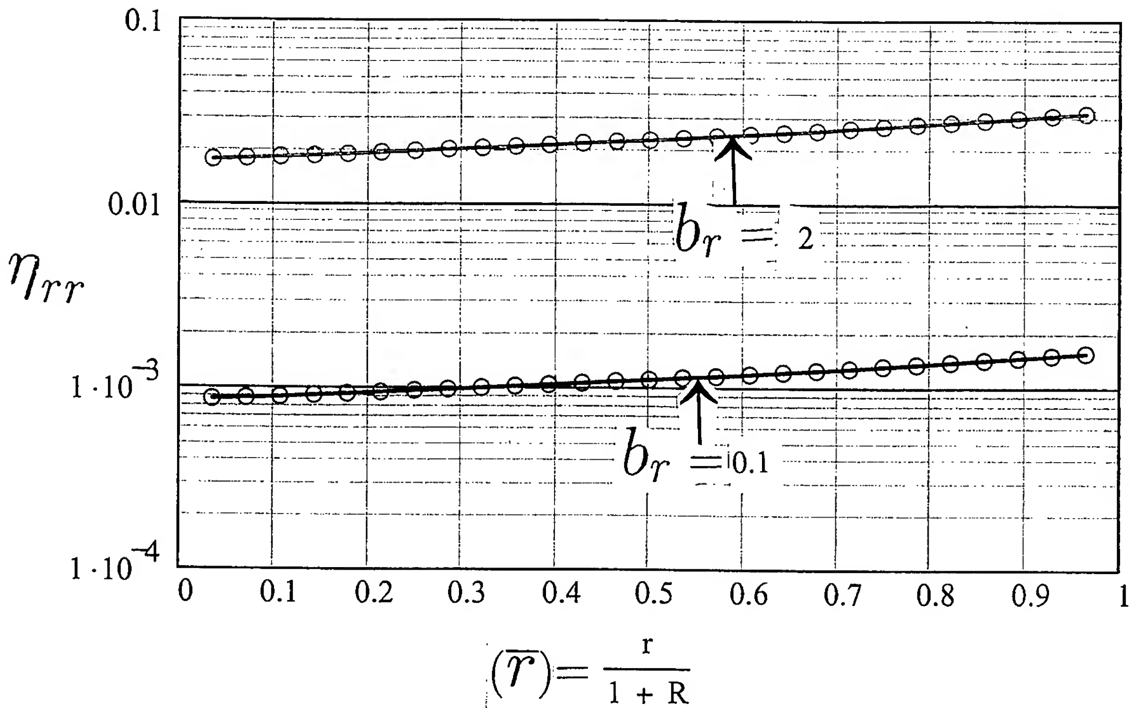

0.1
0.01
$1 \cdot 10^{-3}$
$1 \cdot 10^{-4}$
η_{rr}
$b_r = 2$
$b_r = 0.1$
0
0.1
0.2
0.3
0.4
0.5
0.6
0.7
0.8
0.9
1
$(\overline{r}) = \frac{r}{1 + R}$

Viewgraph 7

Subsequently, without essential loss in generality, it is assumed that $\alpha_r = \alpha$, $\alpha_{cr} = \alpha_c$, $\overline{m}_{cr} = \overline{m}_c$, $\overline{g}_r = \overline{g}$ and $b_r = b$. In this viewgraph the induced loss factor $\eta_s(y)$ is depicted for satellite oscillators that are largely in the form of sprung-masses. Depicted is a situation in which the modal overlap parameter (b) is small compared with unity; $b = 0.1$. The undulations in the induced loss factor $\eta_s(y)$, as a function of (y), is clearly discernible [2]. The mass ratio (M_s / M) is chosen to be 0.1. [This value of (M_s / M) is maintained throughout, where (M_s) is the total mass of the satellite oscillators and (M) is the mass of the master oscillator. Also (R) is maintained at the value of (27) throughout, where (R) is the number of satellite oscillators in the complex. Changes in the value of (M_s / M) and (R) are readily introduced when called for.]

For a modal overlap parameter (b_r) that is less than unity; $b_r < 1$, adjacent satellite oscillators reside outside each other's bandwidths. Consequently, the influence of the satellite oscillators on the response of the master oscillator, as a function of (y); $y = (\omega / \omega_o)$, can be identified individually; each contribution associated with a satellite oscillator stand out prominently from the others.

An example of such an influence in terms of evaluating the induced loss factor $\eta_s(y)$, as a function of (y) with (b_r) less than unity, is depicted in Fig.

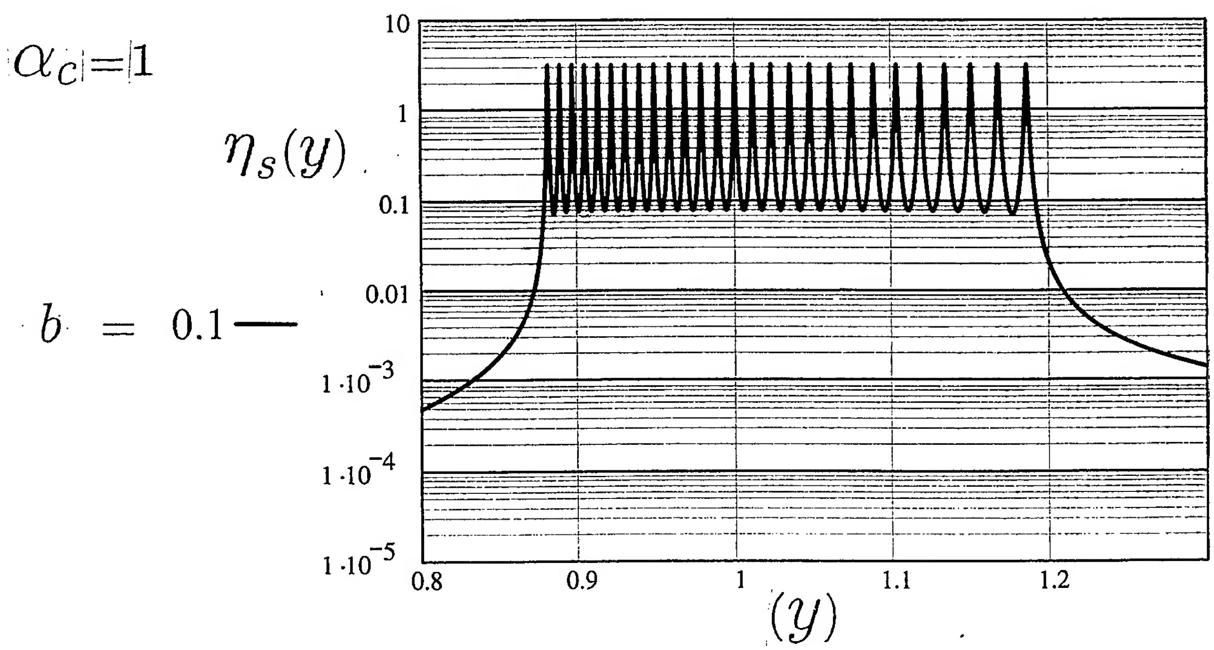

Viewgraph 8

The situation depicted in Viewgraph 7 is repeated here, except that the model overlap factor (b) is increased above unity; $b = 2$. Clearly the induced loss factor $\eta_S(y)$, as a function of (y), is undulations free; the curve is a smooth one. In this viewgraph, as in Viewgraph 7, the mass ratio (M_S / M) is chosen to be (0.1) and the number (R) of satellite oscillators is chosen to be (27).

On the other hand, for a modal overlap parameter (b_r) that exceeds the value of unity; $b_r > 1$, adjacent satellite oscillators reside within each other's bandwidths. Therefore, their influence on the response of the master oscillator is largely continuous as a function of (y); $y = (\omega / \omega_o)$. The more the modal overlap parameter (b_r) exceeds the value of unity, the more the continuity . An example of such an influence, in terms of evaluating the induced loss factor $\eta_s(y)$, as a function of (y) with (b_r) exceeding unity, is depicted in Fig.

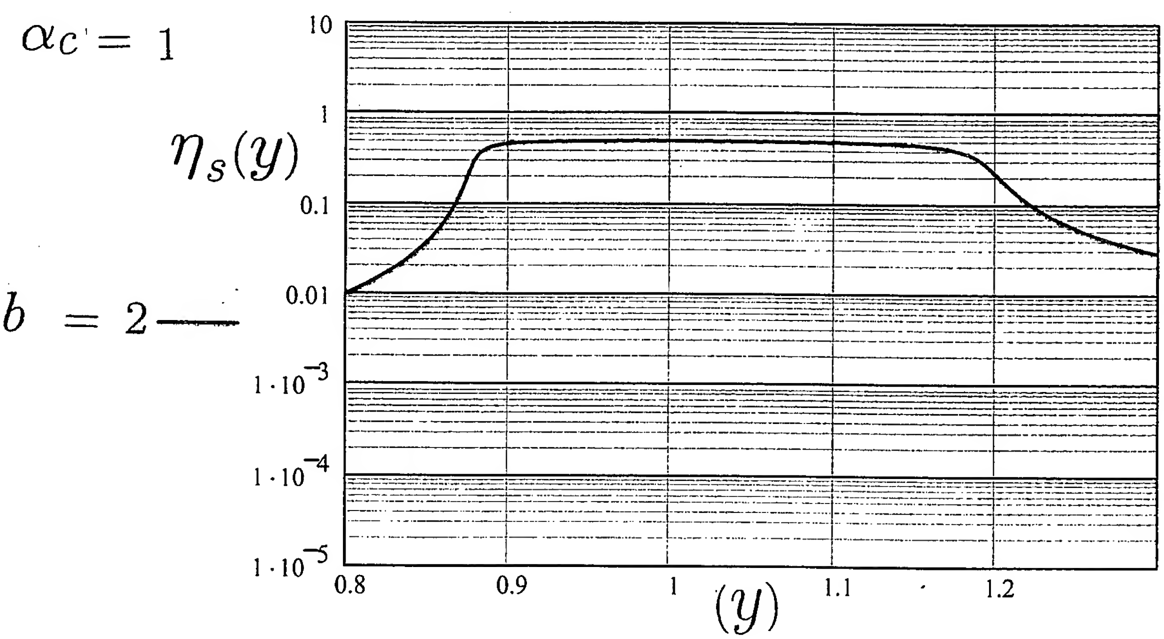

Viewgraph 9a

Stiffness Control Coupling

1. When the curves in Viewgraphs 7 and 8 are directly compared, it is observed that the undulations in the former are mean-valued in the latter [2, 15]. That is, if the undulations in Viewgraph 7 are mean-valued, the resulting smoothed-curve largely duplicates the curve in Viewgraph 8. In that sense, when mean-values are presented, the induced loss factor $\eta_s(y)$ is largely independent of the modal overlap factor (b). (When (b) is large compared with unity, erosion may occur in values of $\eta_s(y)$, especially for small values of (R); the erosion sets in and increases as the values of $[b\ (R+1)^{-1}]$ approach and exceed unity [9, 10]. Some erosion in the value of the induced loss factor $\eta_s(y)$ may be observed at the edges of the normalized frequency range that extends from about $[1 + (\gamma/2)]^{-1/2}$ to $[1 - (\gamma/2)]^{-1/2}$. [cf. Viewgraph 3 and 9d.4.].) In Viewgraphs 7 and 8 the curves pertain to stiffness control couplings that are strong; namely $\alpha_c = 1.0$ $[\alpha = 0.0.]$

2. The overlay of curves is repeated in this viewgraph, except that the coupling, although remaining stiffness control, is lowered in strength to a degree of moderate coupling; namely $\alpha_c = 0.2$ $[\alpha = 0.8.]$ The general features in Viewgraph 9a.2 are similar to those in Viewgraph 9a.1, except that the levels of $\eta_s(y)$ in the former are diminished from those in the latter viewgraph. This decrease is related directly to the difference in the coupling strengths.

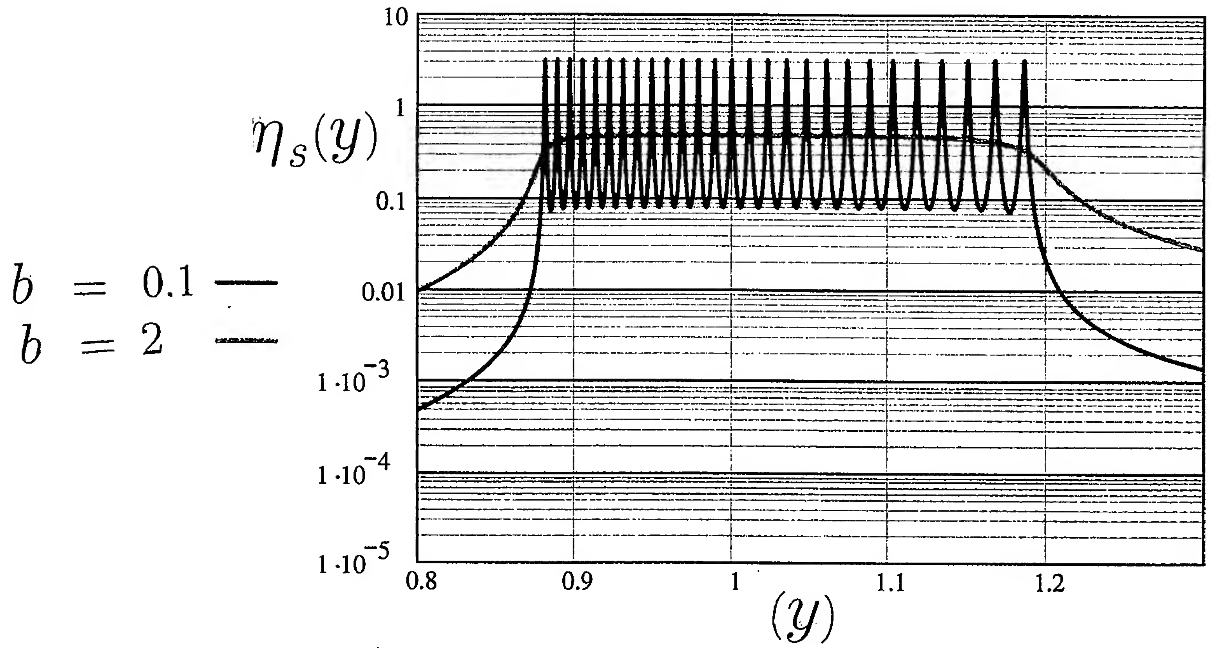

1. (Very) Strong Coupling, $\alpha_c = 1.0$ [$\alpha = 0.0.$]

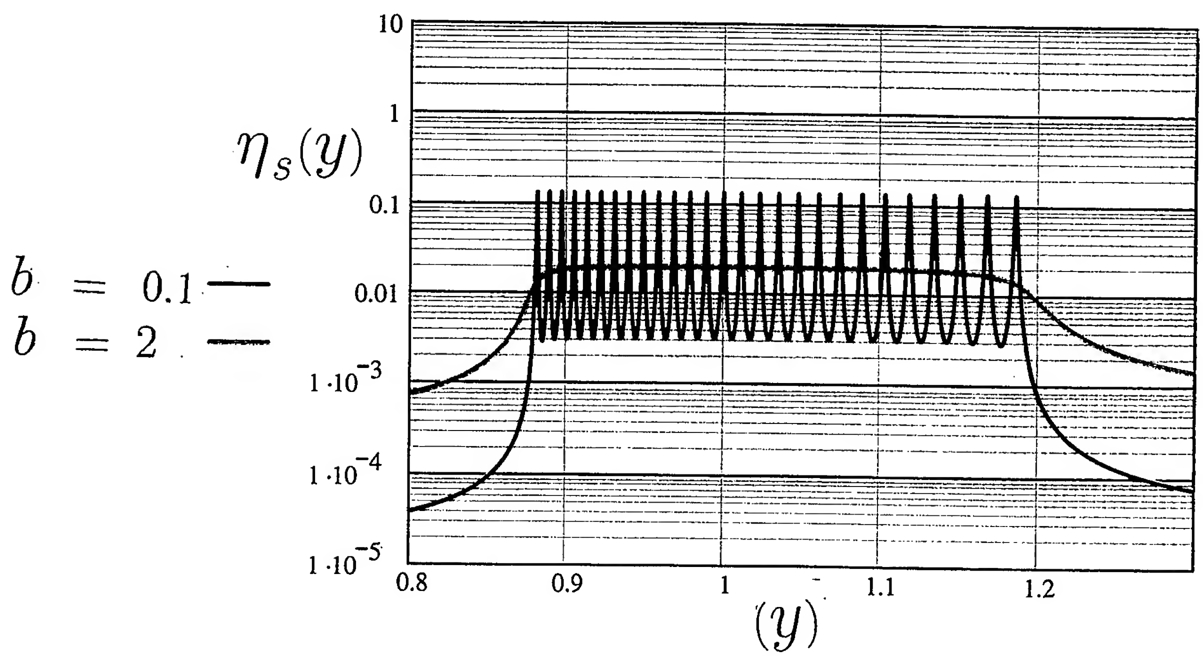

2. Moderate Coupling, $\alpha_c = 0.2$ [$\alpha = 0.8.$]

Viewgraph 9b

Gyroscopic Control Coupling

The format is that of Viewgraph 9a, except that the coupling is gyroscopic in form, rather than of stiffness form. Note the slight slope in the curve over the relevant normalized frequency range. That slope is consistent with the functional dependence of that form of coupling on ($\overline{g}$ / y), rather than simply on ($\overline{g}$).

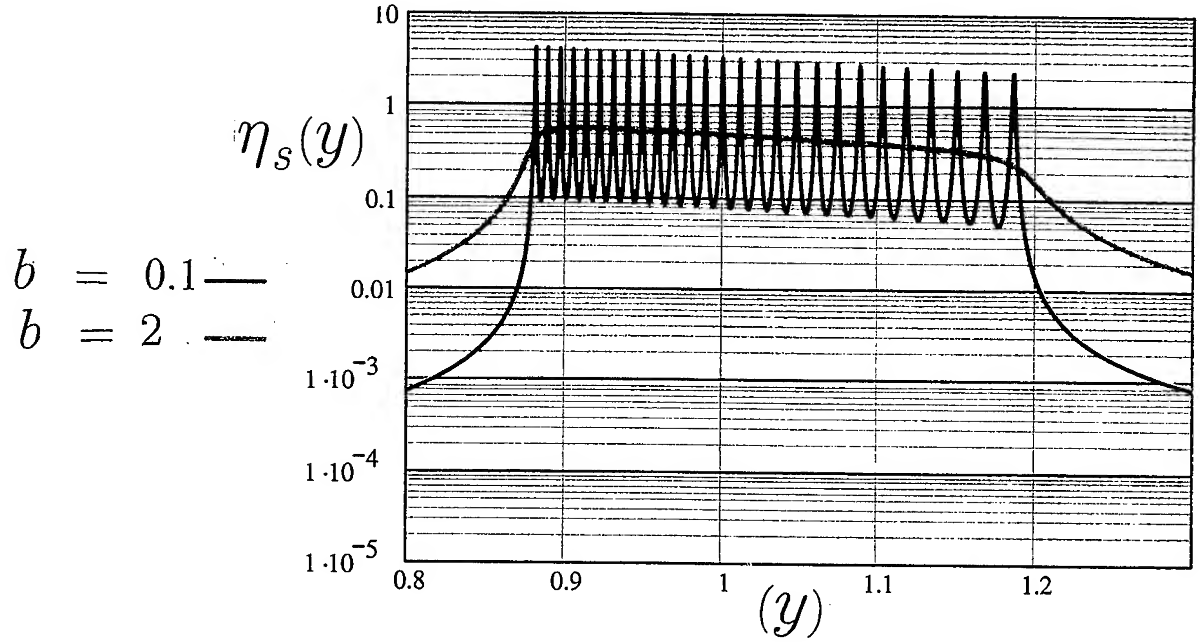

1. (Very) Strong Coupling, $\overline{g} = 1.0$ [$\alpha = 1.0$.]

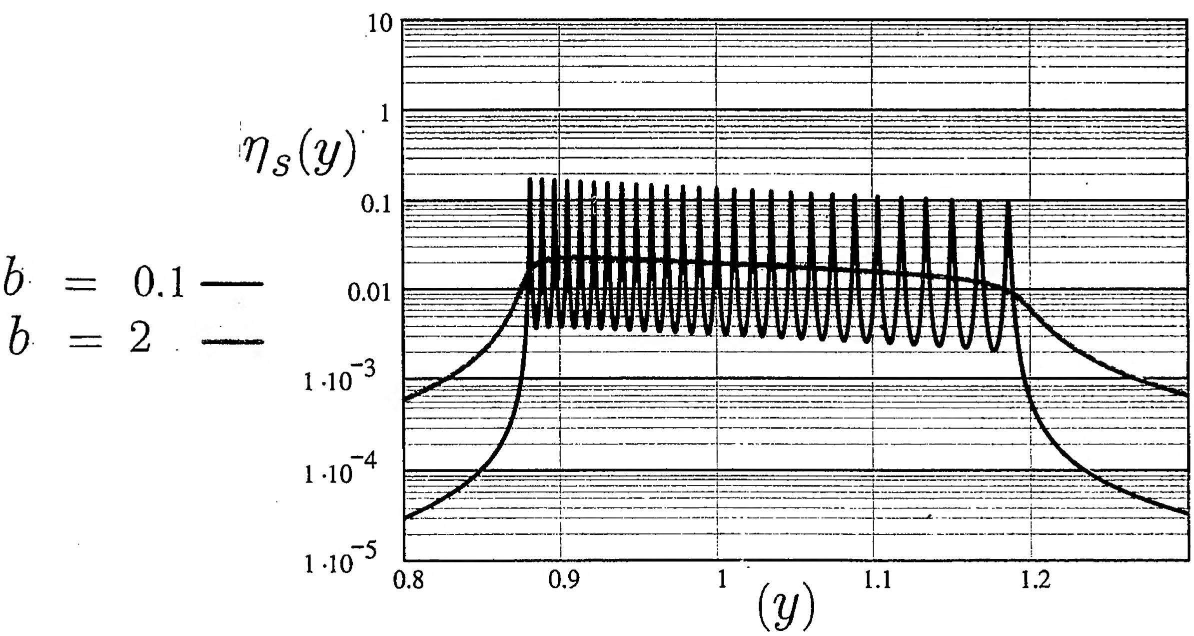

2. Moderate Coupling, $\overline{g} = 0.2$ [$\alpha = 1.0$.]

Viewgraph 9c

Mass Control Coupling

The format is that of Viewgraph 9a, except that the coupling is of mass control in form, rather than of stiffness control form. [cf. Viewgraphs 9d.3 and 12c.]

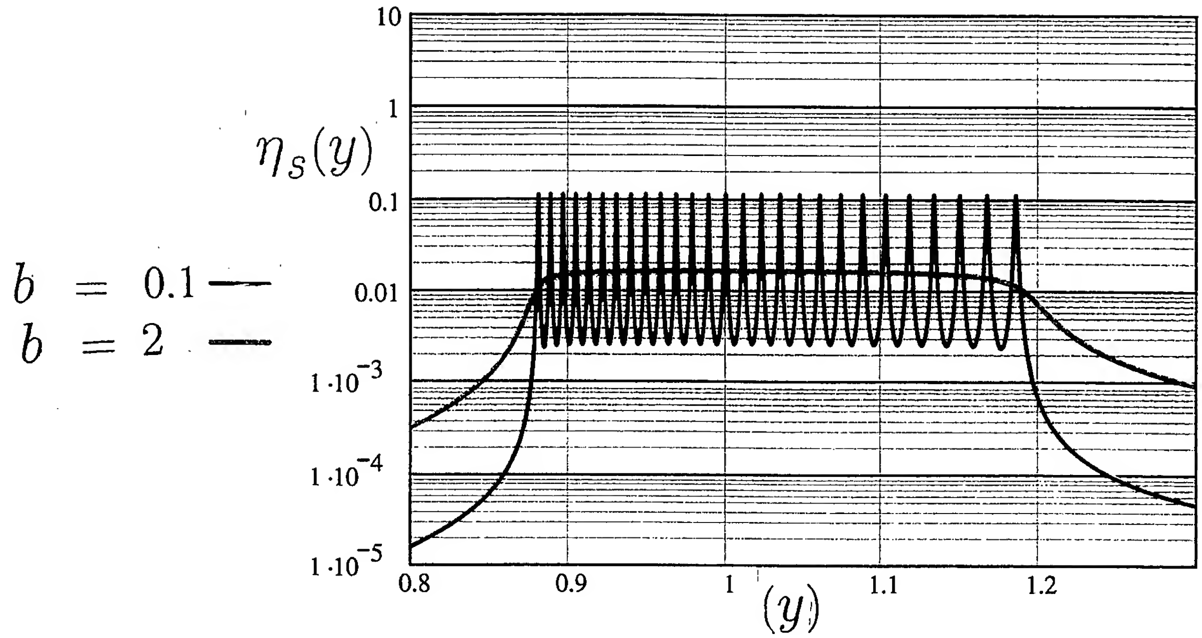

1. Moderate Coupling, $\overline{m_c} = 0.2$ [$\alpha = 1.2.$]

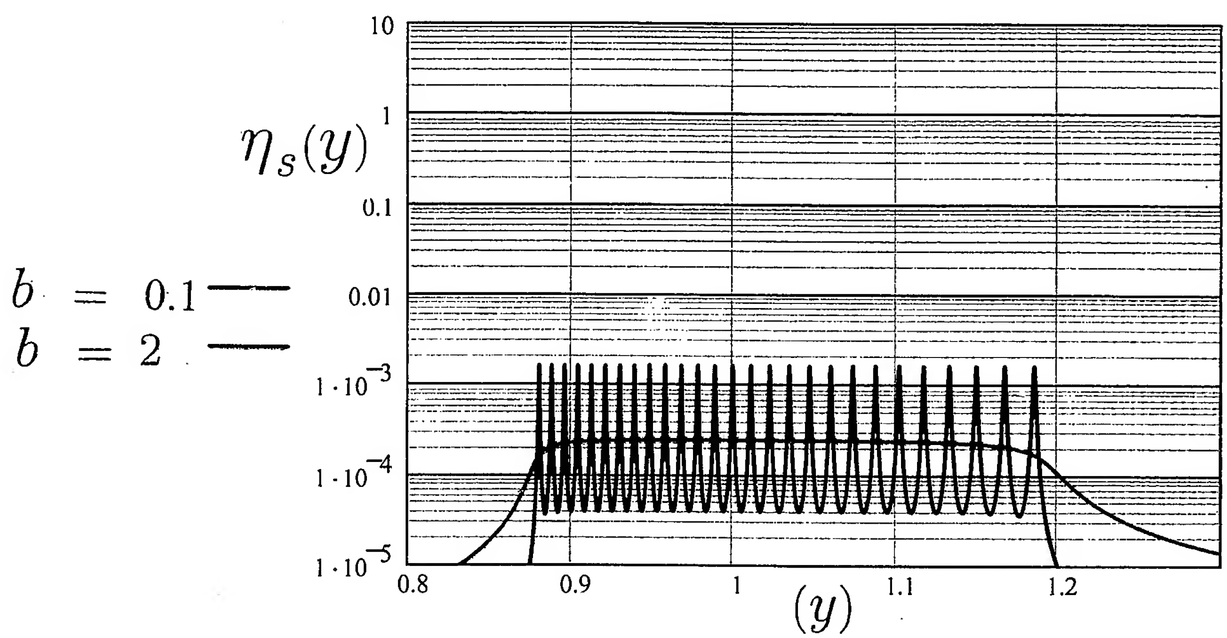

2. Weak Coupling, $\overline{m_c} = 0.0225$ [$\alpha = 1.0225.$]

Viewgraph 9d

Stiffness and Gyroscopic Coupling

The format is that of Viewgraph 9a, except that the coupling is a combination of stiffness and gyroscopic control forms, rather than merely of stiffness control form.

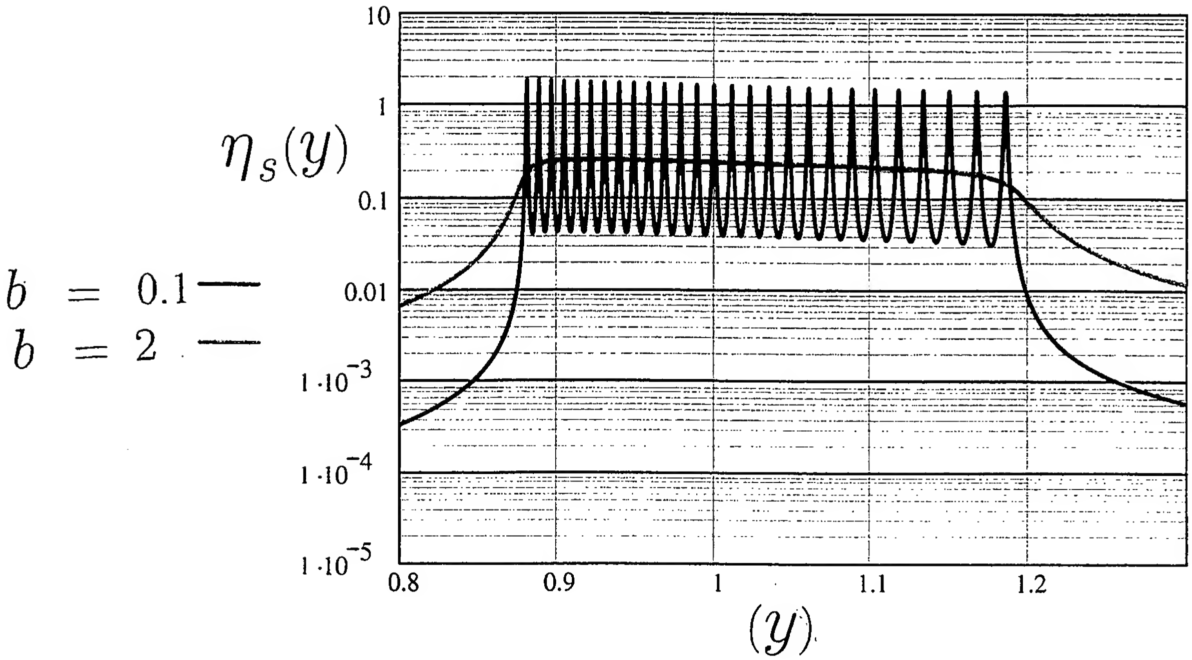

1. Strong Coupling, $\alpha_c = 0.5$; $\vec{g} = 0.5$ [$\alpha = 0.5.$]

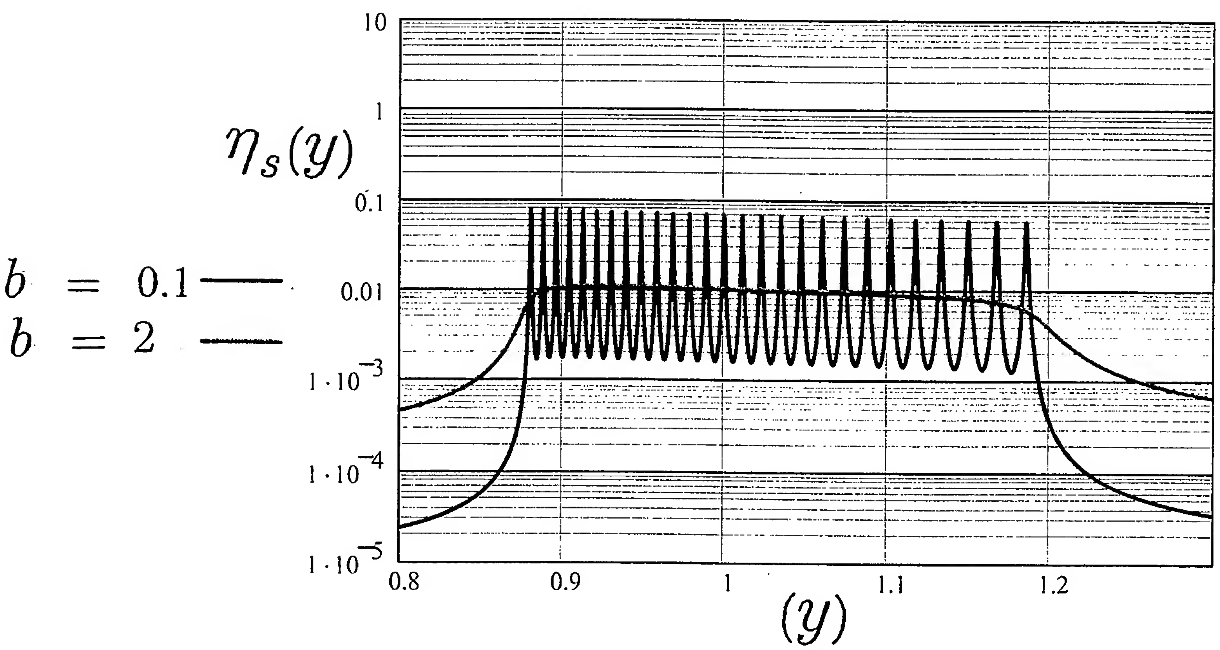

2. Moderate Coupling, $\alpha_c = 0.1$; $\vec{g} = 0.1$ [$\alpha = 0.9.$]

Viewgraph 9d (Continued)

3. Weak coupling is examined in this viewgraph. Again, the significant feature is a reduction in level in $\eta_S(y)$ accompanied by reduction in coupling strength. [cf.. Viewgraphs 9d.1 and 9d.2.]

4. A considerable increase in the modal overlap parameter (b) is examined in this viewgraph; (b) is increased from (0.1) to (10). [cf. Viewgraph 9d.2.] Again, the significant feature is an increasing erosion at the edges of the frequency range. [cf. Viewgraph 9d.2 and 12d.2.] In any case, one should be aware that the value of the induced loss factor $\eta_S(y)$ is largely significant only at and in the vicinity of $y = 1$, where the loss factor in the impedance of the master oscillator has a dominant role to play in the response behavior of this oscillator. It is noted that at this frequency range of $y \simeq 1$, all values of $\eta_S(y)$ are without erosion for $R = 27$.

Note to Viewgraph 9.

Variations on the theme can be readily implemented. However, enough exhibits are presented to acquaint the reader with some of the salient features that underlie all of them.

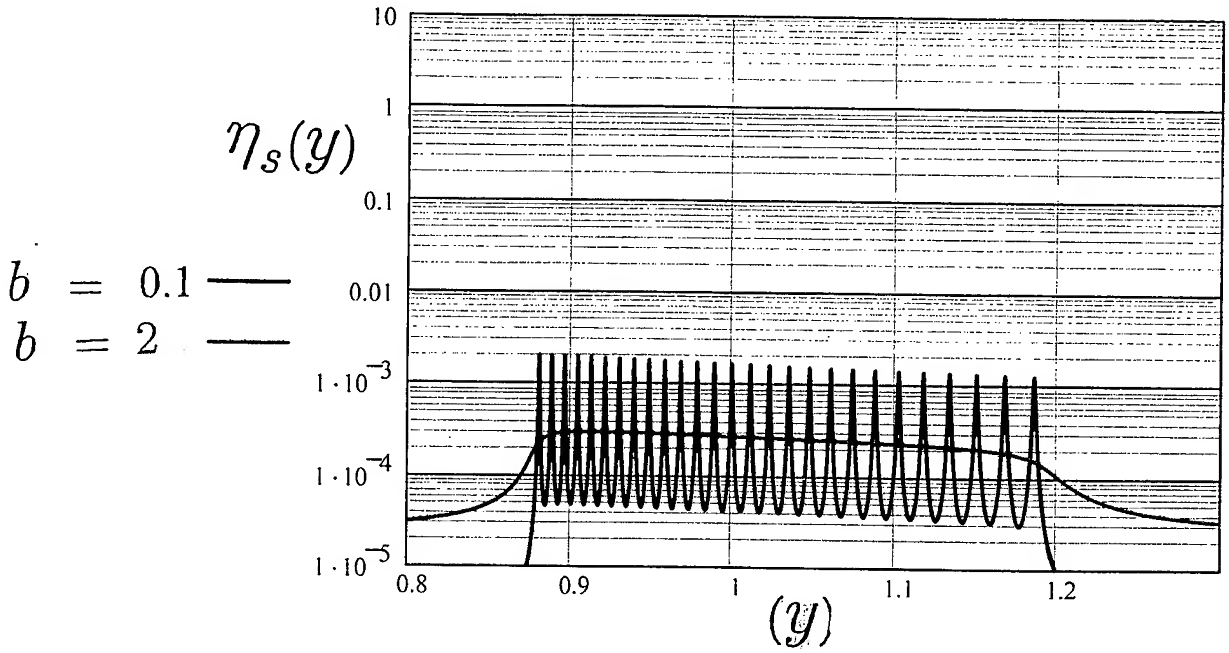

3. Weak Coupling, $\alpha_c = 0.01$; $\overline{g} = 0.02$ [$\alpha = 0.99$.]

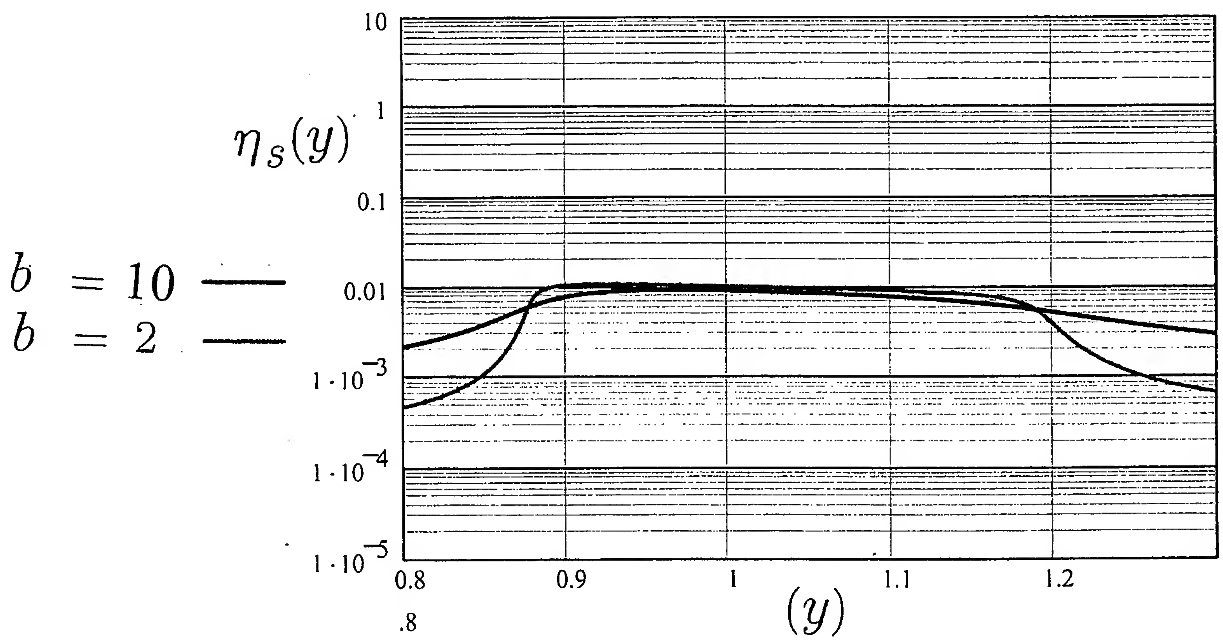

4. Consideration of Edge Erosion

$\alpha_c = 0.1$; $\overline{g} = 0.1$ [$\alpha = 0.9$.]; b = 10 and 2.

Viewgraph 10

The summation in the expression for the induced loss factor $\eta_s(y)$ presented in Viewgraph 2 may be evaluated, to first order of approximation, by replacing the summation by an integration. The prescription for this replacement is stated in this viewgraph. Also stated is the result of the evaluation of the integration under the condition imposed in Viewgraphs 7 and 8. The result is amazingly simple and constitutes the crux of the message in the thesis presented herein.

It is clear that under the definition of (x_r^o), chosen in Viewgraph 3, the range, in the normalized frequency variable (y) for which the result is valid, is stated in the viewgraph. Also given is the condition that $(1 + \overline{m_c}) = (\alpha + \alpha_c)$.

The factor (D) is largely determined by the mass ratio (M_s / M), where (M_s) is the total mass in the satellite oscillators and (M) is the mass of the master oscillator. The term (C) is quadratic in the coupling parameters (α_c), $(\overline{m_c})$ and $(\overline{g})$, with the first two acting coherently. There is a term that is quadratic in a typical loss factor $\eta(y)$ of a satellite oscillator. Thus, only when the coupling parameters are less than this loss factor; $\eta(y) >$ (α_c), $(\overline{m_c})$, $(\overline{g})$, may $\eta_s(y)$ be significantly dependent on $\eta(y)$. However, and in particular, if the satellite oscillators are sprung-masses this dependence vanishes. For some other forms of couplings, this dependence may be significant. One should note, however, that, in general, the inequality placed on $\eta(y)$, with respect to the coupling parameters, requires (very) weak coupling strengths. To make this dependence significant one also requires a special form of coupling, so that (O) is not unusually and simultaneously small; e.g., for a non-stiffness control form of coupling, (O) is identically zero.

$$\sum_{1}^{R} \{ \quad \equiv (y) \int_{z_{\overline{r}}(\overline{\epsilon})}^{z_{\overline{r}}(\overline{R}+\overline{\epsilon})} dz_{\overline{r}}(\overline{r})[f(\overline{r})(R+1)] \ \{$$

$$f(\overline{r})dz_{\overline{r}}(\overline{r}) = d\overline{r} \qquad \overline{r} = r(R+1)^{-1} \quad ;$$

$$\overline{\epsilon} = \epsilon(R+1)^{-1} \quad ; \quad (\overline{R}+\overline{\epsilon}) = (R+\epsilon)(R+1)^{-1}$$

$$\eta_s(y) = D\left[C + O\{\eta(y)\}^2\right]$$

$$D = [\pi/\gamma][M_S/M][1+\overline{m}_C]^{-1} \quad ; \quad \gamma < 1$$

$$C = [\{(\overline{m}_C + \alpha_C)^2\} + \{\overline{g}/y\}^2]$$

$$O = [(1+\overline{m}_C - \alpha_C)\,\alpha_C]$$

$$\eta(y) = b\,[\gamma(\overline{R})(y)^2](R+1)^{-1} \quad ; \quad \gamma(\overline{R}) = [\gamma/(2\overline{R})]$$

$$[1+(\gamma/2)]^{-(1/2)} \leq y \leq [1-(\gamma/2)]^{-(1/2)}$$

$$(1+\overline{m}_C) = (\alpha + \alpha_C)$$

Viewgraph 11

The induced loss factor $\eta_s(y)$, as evaluated by replacing the summation by an integration, is presented for two values of the modal overlap parameter (b); b = 0.1 and 2. The satellite oscillators are largely sprung-masses. One immediately notices that, in the valid normalized frequency range, the results for the two values of (b) are largely independent of (b). These results are then compared with those presented in Viewgraph 9a.1. One may conclude that the results of replacing the summation by an integration, and carrying out the integration to a first order of approximation, is that mean-values only are issued in this evaluation; i.e., the undulations that characterize Viewgraph 7, are suppressed by the mean-value theorem in this viewgraph [2, 15]. In the second of the graphs direct comparison between Viewgraphs 9a.1 and 11.1 is conducted; i.e., in Viewgraph 11.2. It, thus, emerges that the undulations exist only in one of the three curves, showing that the integration invariably yields results that are commensurate with mean-values only and, as such, the results are largely independent of the modal overlap parameter (b). In the normal frequency range of validity, three of the curves largely coincide, not only in level, but in being undulation free.

Interestingly, in the result yielded by replacing the summation by integration there is no sign of erosion in the first order of approximation at the edges of the frequency range. (This is to be expected since the first order of approximation relies, a priori, on small values for the model overlap parameter [2].) An erosion at these edges, however, is observed in the exact evaluation of the summation. [cf.. Viewgraph 9d.] Again, one should be aware, in any case, that the value of the induced loss factor $\eta_s(y)$ is largely significant only at and in the vicinity of y = 1, where the loss factor in the impedance of the master oscillator has a dominant role to play in the response behavior of this oscillator. It is noted that at this frequency range of $y \simeq 1$, all values of $\eta_s(y)$ are without erosion for R = 27. [cf. Viewgraphs 9d.3 and 9d.4.]

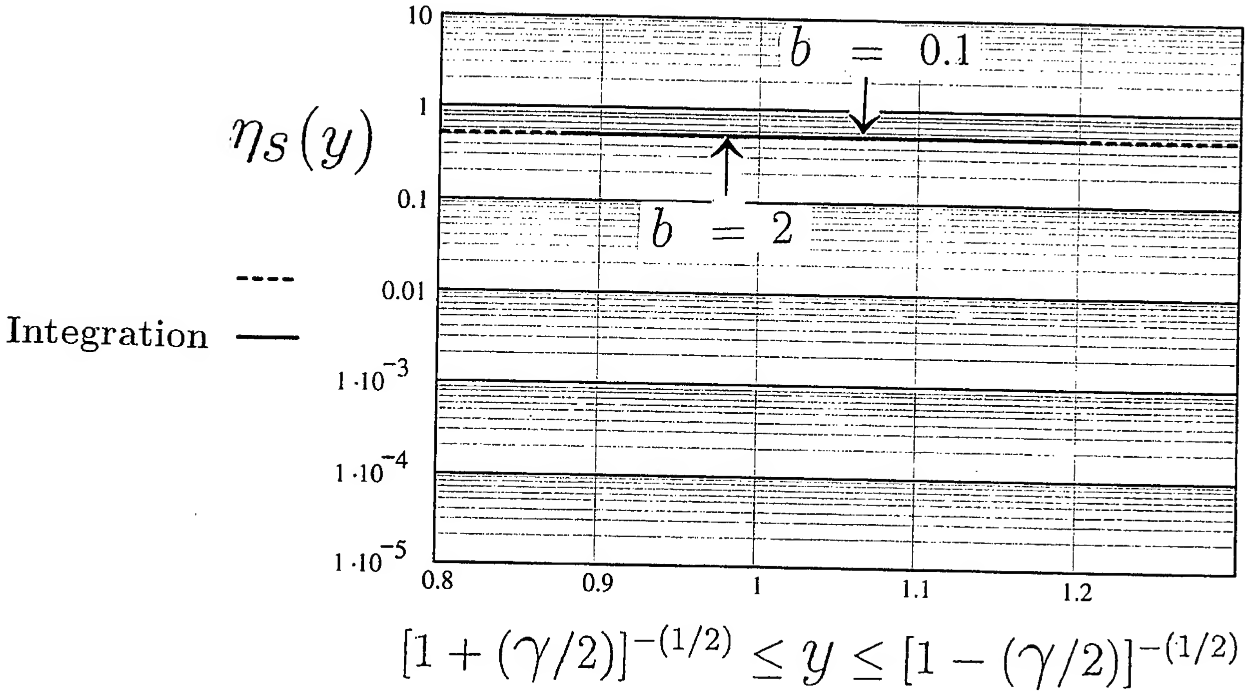

10
1
0.1
0.01
1·10^-3
1·10^-4
1·10^-5
ηs(y)
b = 0.1
b = 2

Integration —
0.8
0.9
1
1.1
1.2
[1 + (γ/2)]^-(1/2) ≤ y ≤ [1 − (γ/2)]^-(1/2)

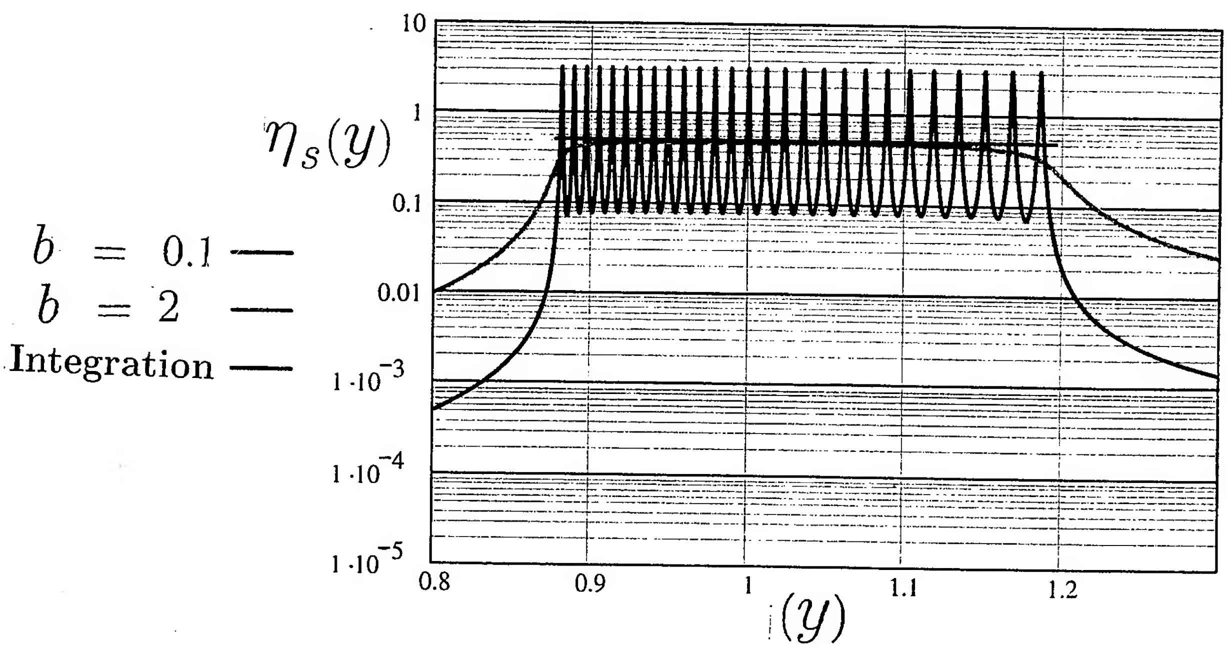

10
1
0.1
0.01
1·10^-3
1·10^-4
1·10^-5
ηs(y)
b = 0.1 —
b = 2 —
Integration —
0.8
0.9
1
1.1
1.2
(y)

Viewgraph 12a

Stiffness Control Coupling

The graph in Viewgraph 11.2 is repeated in the first of this viewgraph; i.e., Viewgraph 12a.1. In this viewgraph the coupling is that of sprung-mass; i.e., $\alpha_c = 1$ [$\alpha = 0.0$.] [cf. Viewgraph 9a.1.]

As in viewgraphs under the designation of 9, several coupling forms and several coupling strengths are depicted in viewgraphs under the designation of 12. Each viewgraph of this series carries two different coupling strengths; the last viewgraph; i.e., Viewgraph 12d, of this series carries three different strengths. [cf .Viewgraphs 9a, 9b, 9c and 9d.] The commonalities and contrasts among these series yield a wealth of information regarding the coupling forms and the coupling strengths in the behavior of this type of complex.

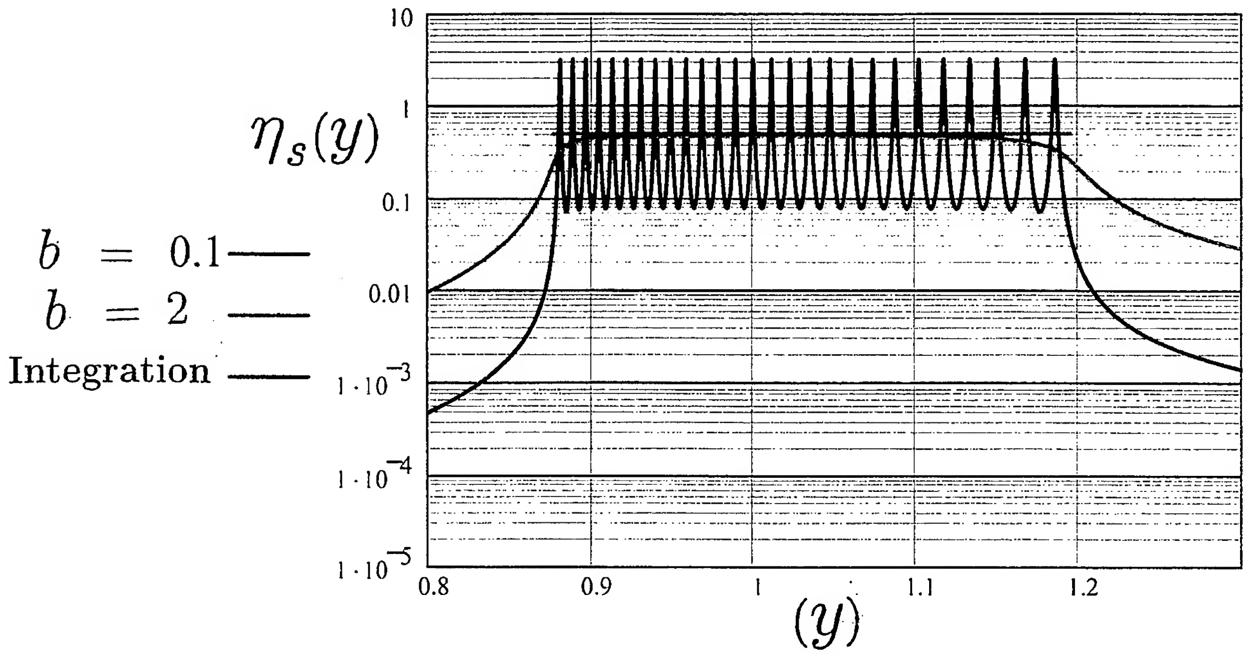

1. (Very) Strong Coupling, $\alpha_c = 1.0$ [$\alpha = 0.0$.]

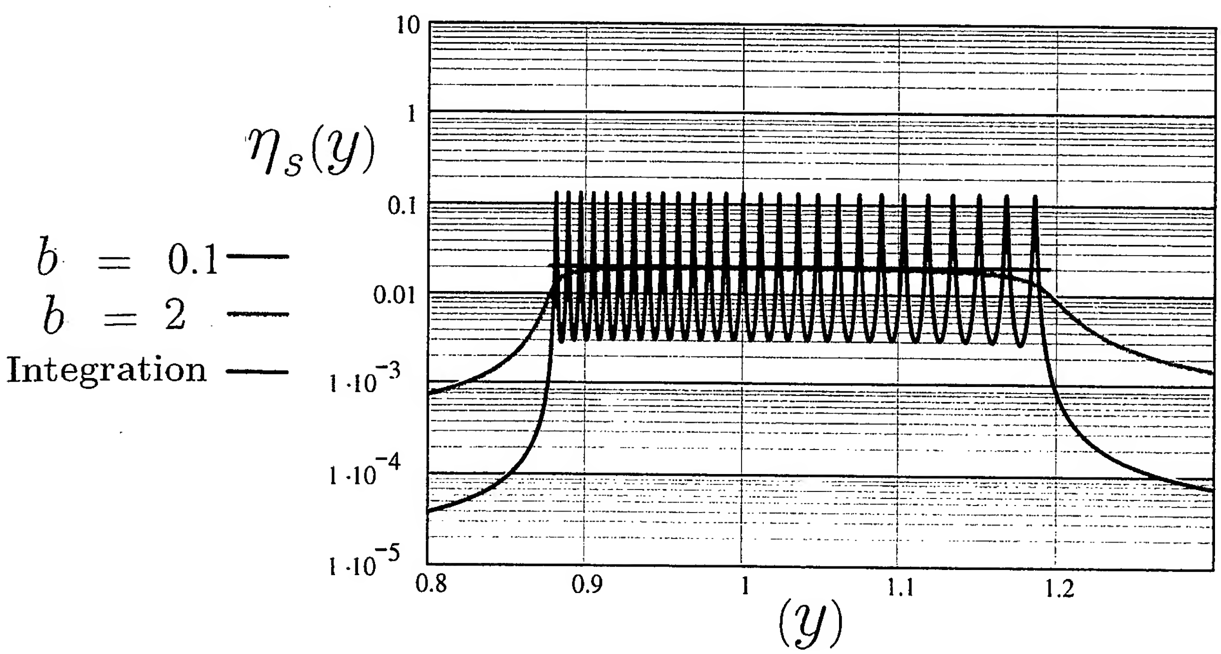

2. Moderate Coupling, $\alpha_c = 0.2$ [$\alpha = 0.8$.]

Viewgraph 12b.

Gyroscopic Control Coupling

[cf. Viewgraph 9b.]

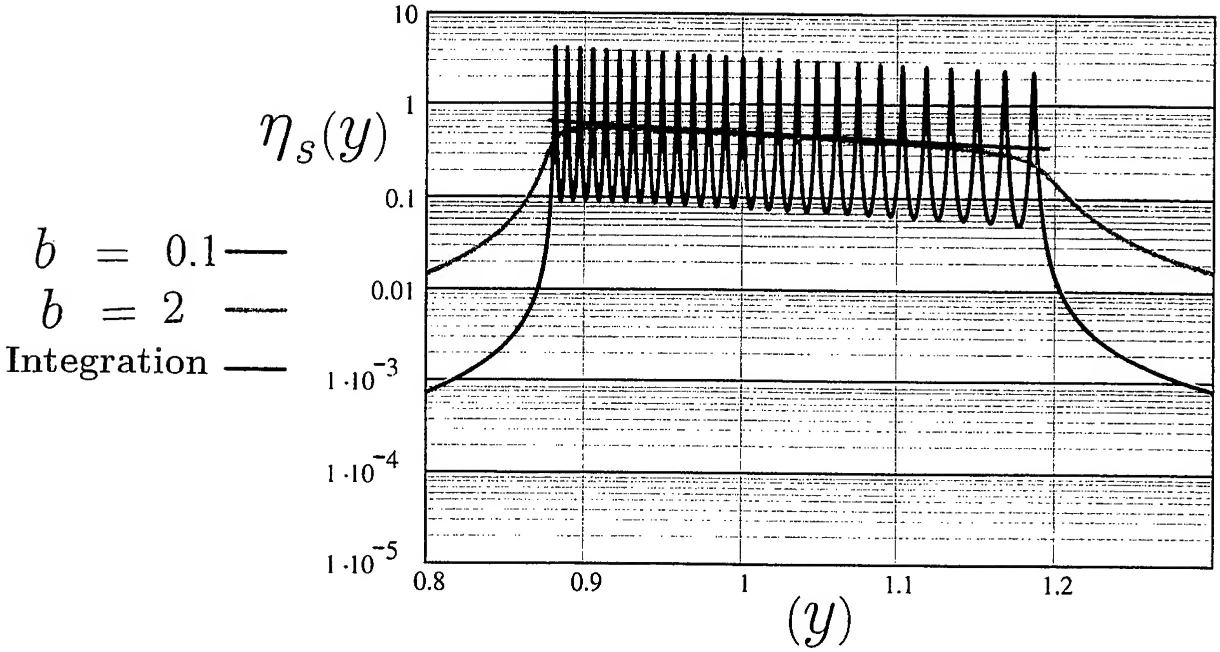

1. (Very) Strong Coupling, $\overline{g} = 1.0$ [$\alpha = 1.0$.]

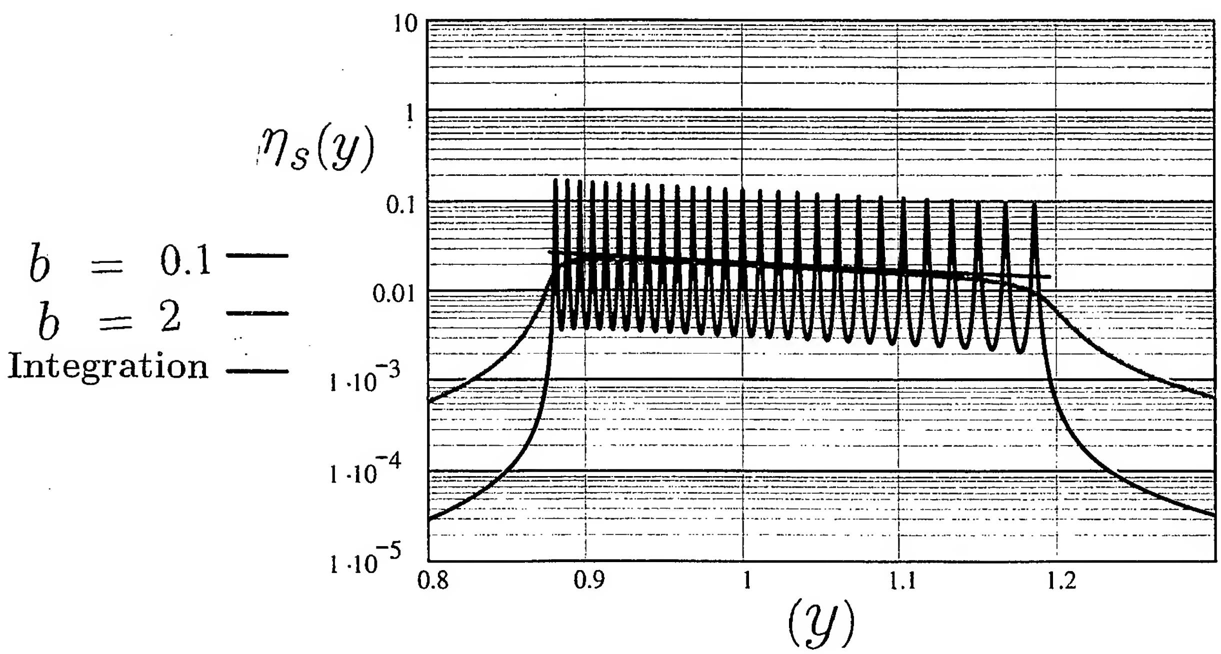

2. Moderate Coupling, $\overline{g} = 0.2$ [$\alpha = 1.0$.]

Viewgraph 12c

Mass Control Coupling

[cf. Viewgraphs 9c and 9d.3.]

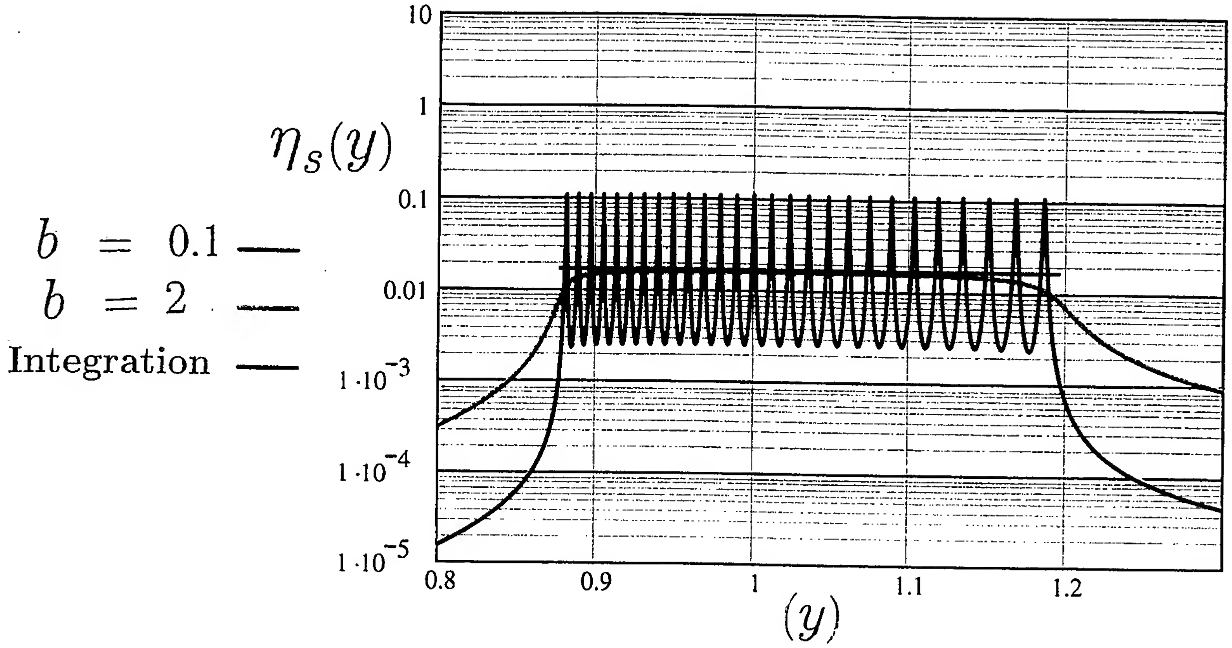

1. Moderate Coupling, $\overline{m}_c = 0.2$ [$\alpha = 1.2.$]

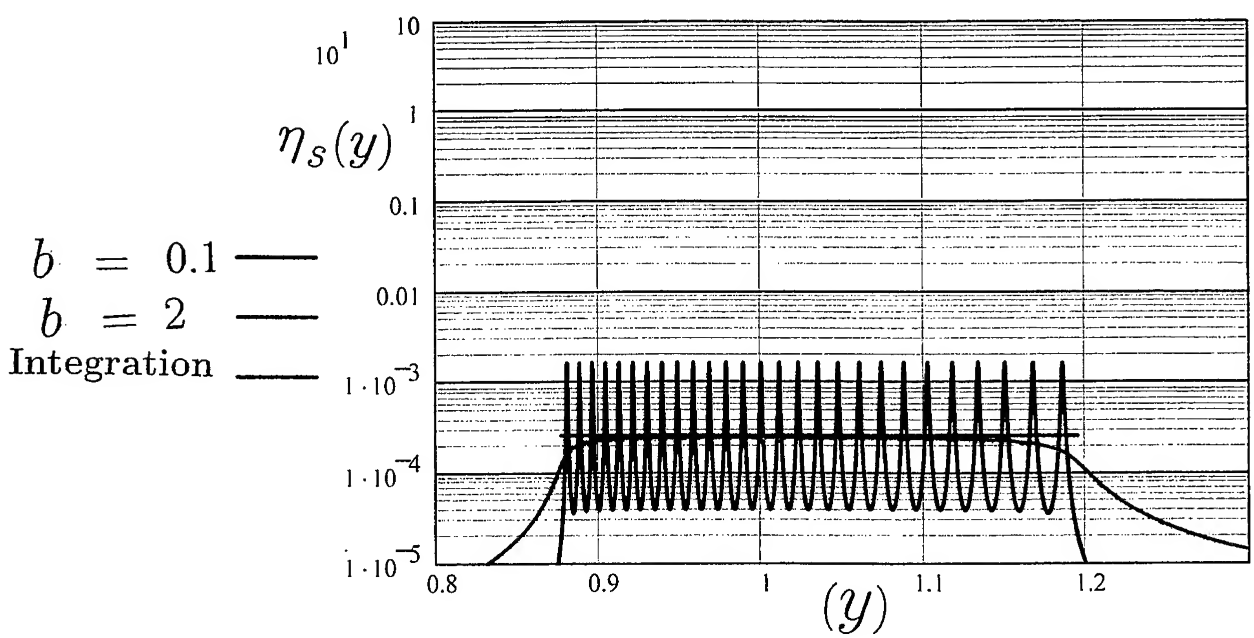

2. Weak Coupling, $\overline{m}_c = 0.0225$ [$\alpha = 1.0225.$]

Viewgraph 12d

Stiffness and Gyroscopic Coupling

[cf. Viewgraph 9d.]

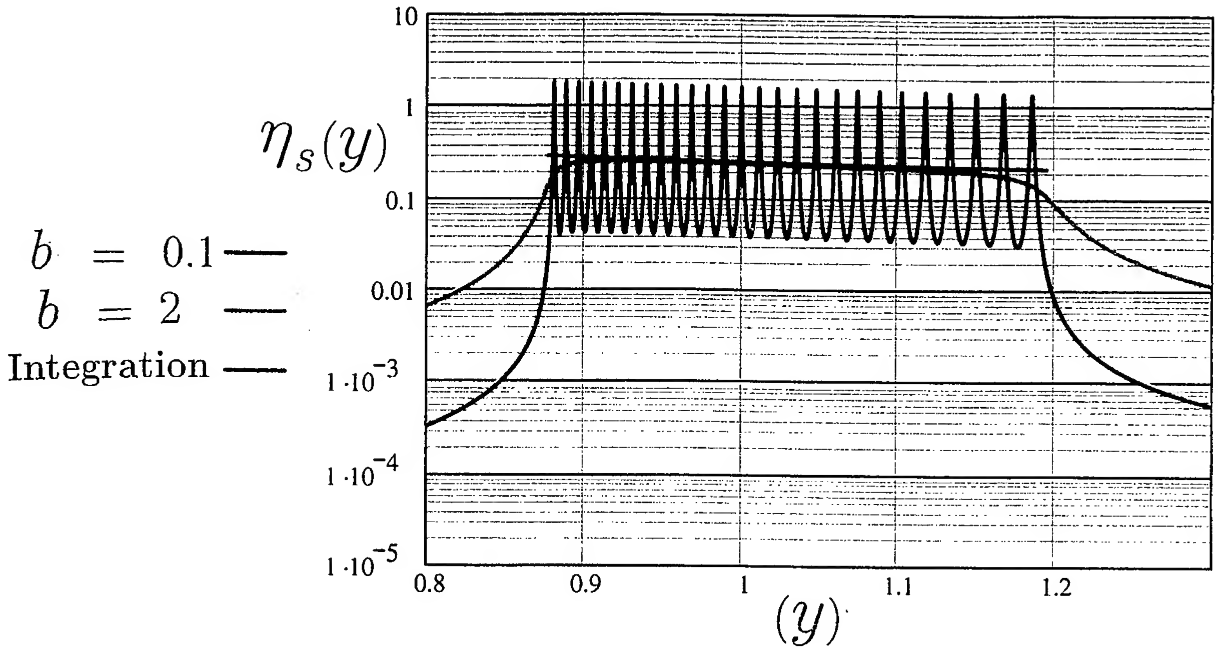

1. Strong Coupling, $\alpha_c = 0.5$; $\overline{g} = 0.5$ [$\alpha = 0.5.$]

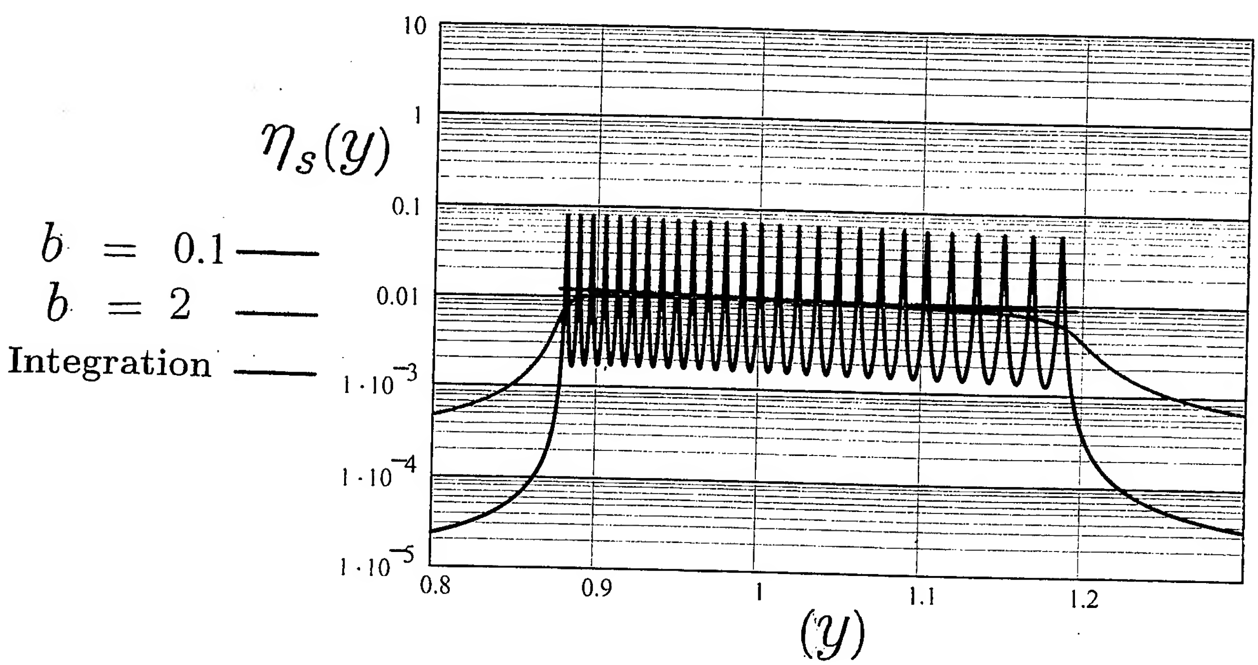

2. Moderate Coupling, $\alpha_c = 0.1$; $\overline{g} = 0.1$ [$\alpha = 0.9.$]

Viewgraph 12d (Continued)

3. Weak coupling is examined in this viewgraph. Again, the significant feature is a reduction in level in $\eta_s(y)$ accompanied by reduction in coupling strength. [cf.. Viewgraphs 9d (Continued) and 12c.2.]

4. A considerable increase in the modal overlap parameter (b) is examined in this viewgraph; (b) is increased from (0.1) to (10). [cf. Viewgraph 9d (Continued) and 12c.2.] Again, the significant feature is an increasing erosion at the edges of the frequency range. [cf. Viewgraph 9d (Continued) and 12c.2.] In any case, one should be aware that the value of the induced loss factor $\eta_s(y)$ is largely significant only at and in the vicinity of $y = 1$, where the loss factor in the impedance of the master oscillator has a dominant role to play in the response behavior of this oscillator. It is noted that at this frequency range of $y \simeq 1$, all values of $\eta_s(y)$ are without erosion for $R = 27$.

Note to Viewgraph 12.

Variations on the theme can be readily implemented. However, enough exhibits are presented to acquaint the reader with some of the salient features that underlie all of them.

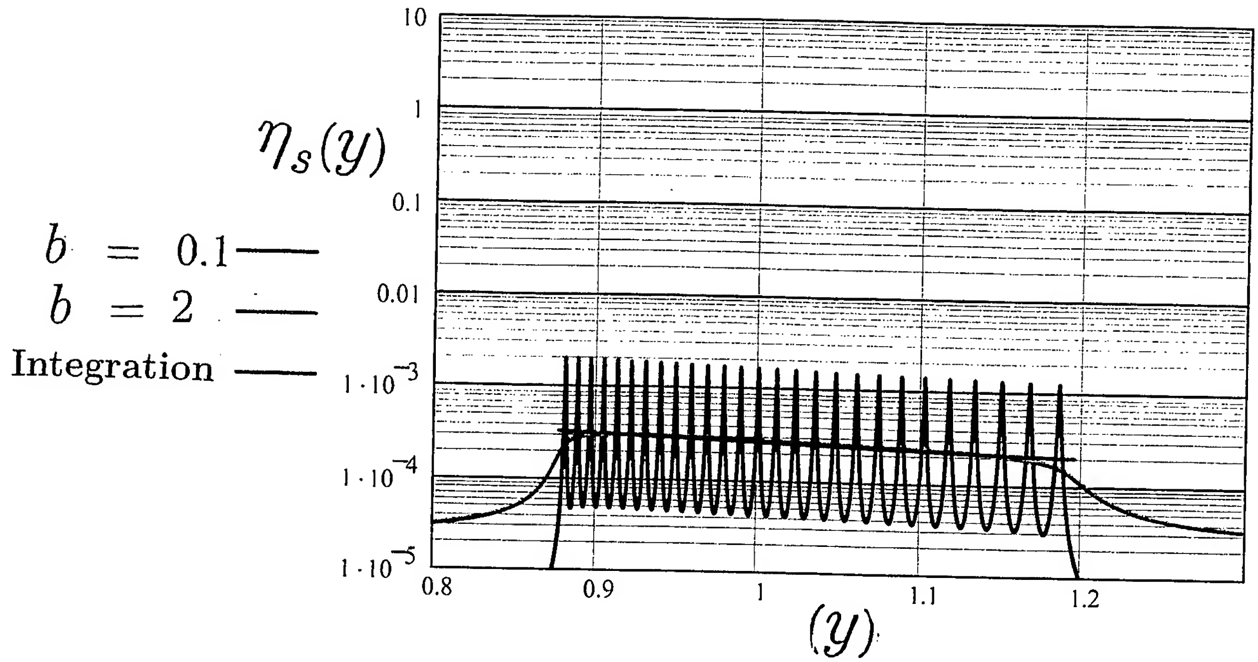

3. Weak Coupling, $\alpha_c = 0.01$; $\overline{g} = 0.02$ [$\alpha = 0.99.$]

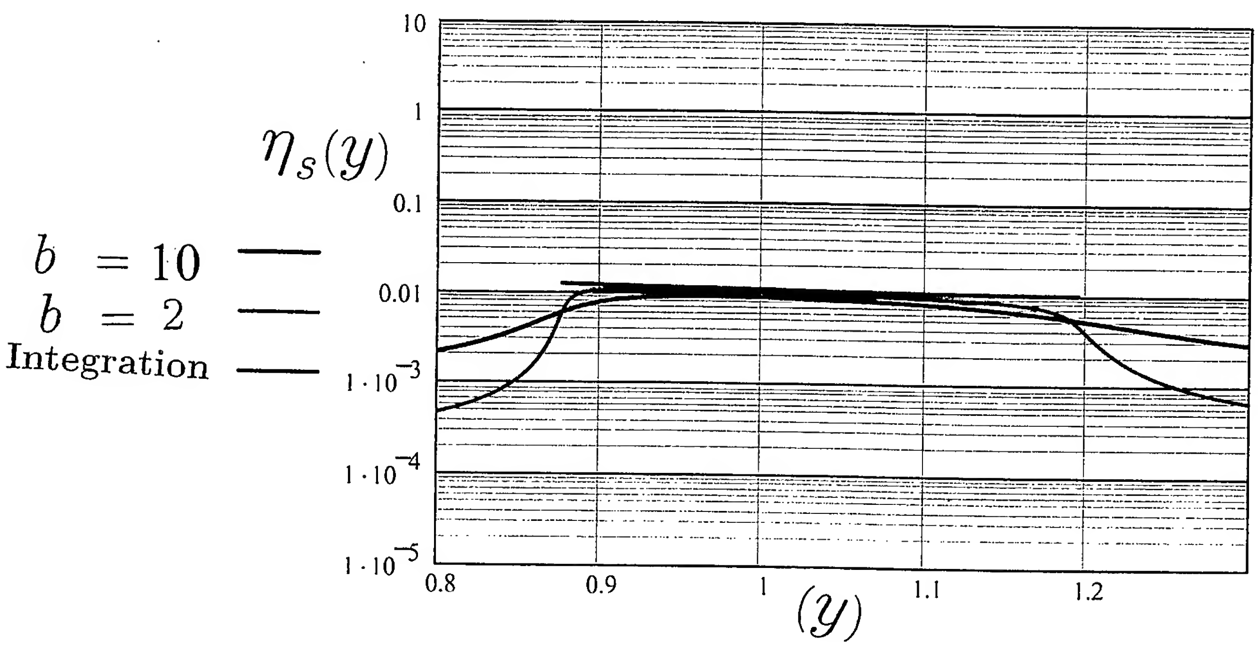

4. Consideration of Edge Erosion

$\alpha_c = 0.1$; $\overline{g} = 0.1$ [$\alpha = 0.9.$]; b = 10 and 2.

References

1. G. Maidanik, "Supplementarity of damping and isolation and the invasion of humane aliens", 1998, NSWCCD-70-TR-1998/227.

2. G. Maidanik, "Induced damping by a nearly continuous distribution of nearly undamped oscillators: Linear Analysis" 2000, Journal of Sound and Vibration. Soon to appear in publication.

3. R. H. Lyon, *Statistical Energy Analysis of Dynamic Systems: Theory and Application*, 1975, MIT, Cambridge; and R. H. Lyon and R. G. Dejung, *Theory and Application of Statistical Energy Analysis*, 1995, Butterworth-Heinemann, Boston.

4. G. Maidanik, "Response of coupled dynamic systems" 1976, Journal of Sound and Vibration, **46**, 561-583.

5. G. Maidanik, "Power dissipation in a sprung mass attached to a master structure," 1995, Journal of the Acoustical Society of America, **98**, 3527-3533.

6. A. Pierce, V. W. Sparrow and D. A. Russell, "Fundamental structural-acoustic idealization for structures with fuzzy internals," 1995 Journal of Acoustics and Vibration, **117**, 339-348.

7. M. Strasberg and D. Feit, "Vibration damping of large structures by attached small resonant structures," 1996, Journal of the Acoustical Society of America, **99**, 335-344.

8. R. L. Weaver, "Mean and mean-square responses of a prototypical master/fuzzy structure," 1996, Journal of the American Society of America, **99**, 2528-2529.

References (Continued)

9. M. J. Brennan, "Wideband vibration neutralizer," 1997, Noise Control Engineering Journal, **45**, 201-207.

10. G. Maidanik and K. J. Becker, "Noise control of a master oscillator coupled to a set of satellite harmonic oscillators," 1998, Journal of the Acoustical Society of America, **104**, 2628-2637; "Characterization of multiple-sprung mass for wideband noise control," 1999, Journal of the Acoustical Society of America, **106**, 3119-3127.

11. R. J. Nagem, I. Veljkovic and G. Sandri, "Vibration damping by a continuous distribution of undamped oscillators," 1997, Journal of Sound and Vibration, **207**, 429-434.

12. T. L. Smith, K. Rao and I. Dyer, "Attenuation of plate flexural waves by a layer of dynamic absorbers," 1986, Noise Control Engineering Journal, **26**, 56-60.

13. G. Maidanik and J. Dickey, "Singly and regularly ribbed panels," 1988, Journal of Sound and Vibration, **123**, 309-314.

14. Yu. A. Kobelev, "Absorption of sound waves in a thin layer," 1987, Soviet Physics Acoustics, **33**, 295-296.

15. E. Skudrzyk, "The mean-value method of predicting the dynamic response of complex vibrators," 1980, Journal of the Acoustical Society of America, **67**, 1105-1135.

INITIAL DISTRIBUTION

Copies			
3	NAVSEA 05T2		
	1	Taddeo	
	1	Biancardi	
	1	Shaw	
5	ONR/ONT		
	1	334	Tucker
	1	334	Radlinski
	1	334	Vogelsong
	1	Library	
4	NRL		
	1	5130	Bucaro
	1	5130	Williams
	1	5130	Photiadis
	1	Library	
4	NUWC/NPT		
	1	Sandman	
	1	3332 Lee	
	1	Library	
2	DTIC		
2	Johns Hopkins University		
	1	Green	
	1	Dickey	
3	ARL/Penn State University		
	1	Burroughs	
	1	Hwang	
	1	Hambric	
1	R. H. Lyon		
	1	Lyon	
1	Cambridge Collaborative		
	1	Manning	

Copies		
1	Catholic Univ. of Am. Eng. Dept.	
	1	McCoy
2	Boston University	
	1	Pierce
	1	Barbone
1	Penn State University	
	1	Koopmann
2	Virginia Tech	
	1	Knight
	1	Fuller

CENTER DISTRIBUTION

Copies	Code	Name
1	011	Corrado
1	0112	Barkyoumb
1	0112	Halsall
1	20	Keane
1	26	Everstine
1	70	Covich
1	701	Sevik
1	7014	Fisher
1	7020	Strasberg
1	7030	Maidanik
1	7200	Shang
1	7205	Dlubac

INITIAL DISTRIBUTION (Continued)

Copies		
1	Cambridge Acoustical Associated	
	1	Garrelick
1	J. G. Engineering Research	
	1	Greenspan
1	MIT	
	1	Dyer
4	Individual Subscribers	
	1	Panzer
	1	Sharp
	1	Himelblau
	1	Matteo

CENTER DISTRIBUTION

Copies	Code	Name
1	7207	Becker
3	7220	Carroll Niemiec Vasudevan
2	7250	Bowers Maga
1	842	Graesser
2	3421	(TIC-Carderock)